

Influence of the inhomogeneous strain relaxation on the optical properties of etched quantum wires

Y. M. Niquet

*CEA-CNRS Joint Group "Microstructures de Semiconducteurs II-VI," Laboratoire de Spectrométrie Physique, Université J. Fourier, Grenoble I, Boîte Postale 87, 38402 Saint Martin d'Hères, France
and Institut d'Electronique et de Microélectronique du Nord, Département ISEN, Boîte Postale 69, F-59652 Villeneuve d'Ascq Cedex, France*

C. Priester

Institut d'Electronique et de Microélectronique du Nord, Département ISEN, Boîte Postale 69, F-59652 Villeneuve d'Ascq Cedex, France

H. Mariette

CEA-CNRS Joint Group "Microstructures de Semiconducteurs II-VI," Laboratoire de Spectrométrie Physique, Université J. Fourier, Grenoble I, Boîte Postale 87, 38402 Saint Martin d'Hères, France

(Received 13 September 1996)

Inhomogeneous strain relaxation in quantum wires etched from biaxially strained quantum wells is calculated. Characteristic features of the strain field are systematically discussed as a function of wire dimensions and illustrated with various semiconductor systems either under compressive or tensile strain. We provide a general relaxation curve. The shift of the band-gap energy in nanostructures due to the calculated strain field is then predicted and compared to data obtained from optical spectroscopy experiments.

[S0163-1829(97)50212-8]

Strain relaxation is expected to play an important role in quantum wires (QWRs) etched from quantum wells (QWs) that are under biaxial strain due to the lattice mismatch with the underlying substrate (or buffer layer). These structures undergo a partial elastic relaxation in the vicinity of the sidewalls created by the patterning process, distorting the initial uniform strain state. This distortion can affect the properties of the QWR depending on the lateral size of the wire as compared to the thickness of the strained QW. Some of the optical results for semiconductor QWRs—such as energy shifts of the optical transitions—have been qualitatively related to such relaxation phenomena.^{1,2} Simple analytical solutions assuming a homogeneous strain in the wire have been used to account for experimental data³⁻⁵ *a posteriori*, without *predicting* strain relief in the wire. More recently, calculations using continuum elasticity theory were reported for several structures.⁶ However, no quantitative studies have been carried out so far to predict the influence of elastic behavior on the electronic properties of etched QWRs. This is the purpose of this work.

First, we calculate atomic positions and strain fields in actual etched QWRs, taking into account inhomogeneous strain relaxation in the system. Characteristic features about strain relaxation in QWRs are discussed as a function of wire dimensions and illustrated with various semiconductor QWRs either under compressive or tensile strain. We provide a *general relaxation curve* which can be applied to very numerous systems. Band-gap energy shifts produced by the calculated strain field in these structures are then estimated and compared to experiments when available.

Strain fields in relaxed QWRs are calculated within Keating's valence force field framework.^{7,8} In this model, the elastic strain energy depends on geometric deformations of

bonds (bond bending and bond stretching) that each atom makes with its four nearest neighbors. Thus, we can obtain the atomic positions in the whole structure by finding the minimum energy configuration as the wire is allowed to relax an initial biaxial strain. We consider here a periodic array of wires of infinite length and have neglected surface reconstruction on sidewalls.

This calculation is developed for various QWRs etched from single [001] QWs under either compressive or tensile strain. The growth axis is denoted $z=[001]$, the in-plane directions $x=[1\bar{1}0]$ and $y=[110]$. Note that x and y are not the cubic directions. Before etching, the well is under biaxial strain, the lattice mismatch in-plane deformations $\epsilon_{xx} = \epsilon_{yy} = \epsilon_{\parallel}$ being imposed by a buffer. After etching of wires oriented along the [110] direction, the wires can relax their strain by the two lateral edges on which stress vanishes. Therefore, only ϵ_{yy} remains fixed by the buffer, since the wires are very long. We have investigated especially the case of three compressive semiconductor QWRs on which numerous experimental data are available, namely CdTe QW with $\text{Cd}_{0.88}\text{Zn}_{0.12}\text{Te}$ barriers and buffer⁵ ($\epsilon_{\parallel} = -0.73\%$), $\text{Zn}_{0.80}\text{Cd}_{0.20}\text{Se}$ QW with ZnSe barriers and buffer^{2,4,9} [blue laser system¹⁰ ($\epsilon_{\parallel} = -1.34\%$)], and $\text{In}_{0.18}\text{Ga}_{0.82}\text{As}$ with GaAs barriers¹¹ ($\epsilon_{\parallel} = -1.28\%$). As a case of tensile strain, ZnTe QW between fully relaxed $\text{Zn}_{0.80}\text{Mg}_{0.20}\text{Te}$ layers is also considered ($\epsilon_{\parallel} = +1.03\%$), experimental work on this new system being underway. All lattice and elastic constants were taken from Ref. 8 for telluride and arsenide systems, and from Ref. 4 for selenide systems QWRs.

Results for 80 nm wide CdTe and ZnTe QWRs with 10 nm thick QWs are given in Figs. 1 and 2. Since atomic displacements remain small compared to the wire dimen-

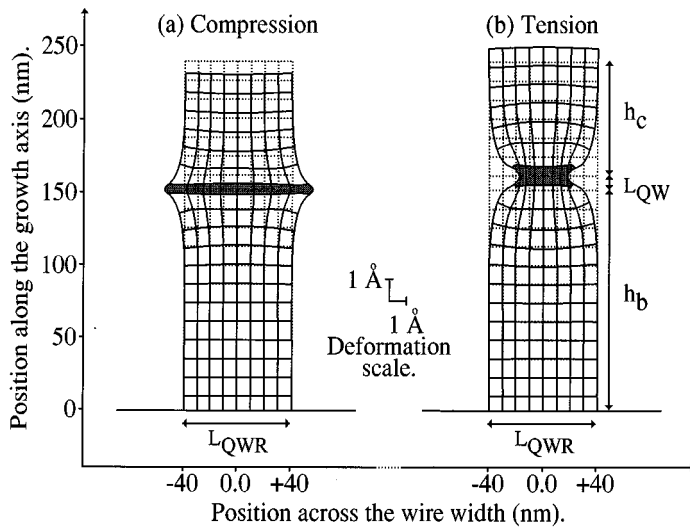


FIG. 1. Position of some lattice planes in a CdTe QWR under compression (a) and in a ZnTe QWR under tension (b) before etching (dashed lines) and after etching (solid lines). The two wells appear in gray. Atomic displacements have been exaggerated so that the real distance between one dashed intersection and the corresponding solid one must be read on the “deformation scale.”

sions, the deformations have been exaggerated in Fig. 1. This figure shows clearly how wells relax strains through the free surfaces created by the etching. The CdTe QW under compression pushes the edges 1.25 \AA outwards, dragging the two barriers with it [Fig. 1(a)], whereas the ZnTe QW under tension pulls wire edges 1.70 \AA inwards [Fig. 1(b)]. The strain component ϵ_{xx} and shear component ϵ_{zx} are plotted on the entire CdTe $\text{Cd}_{0.88}\text{Zn}_{0.12}\text{Te}$ wire in Fig. 2. The strain component ϵ_{xx} [Fig. 2(a)] exhibits a strong gradient in the well, since it decreases rapidly close to the sidewalls, but the strain is partly relaxed even in the center of the wire. This is also illustrated in Fig. 3 for $\text{Zn}_{0.80}\text{Cd}_{0.20}\text{Se}$ QWRs with 10 nm thick QWs and lateral widths within the range 80–320 nm.

As QWs relax their strains, they drag the barriers and thus induce deformations in these layers, which accumulate elastic strain energy and hence limit the relaxation in the well. Due to lattice commensurability, the inhomogeneous well relaxation induces an inhomogeneous deformation in the barriers. The more distorted parts are close to the sidewalls and give rise to a strong shear component ϵ_{zx} [Fig. 2(b)] and to a lattice plane bending, as is clearly shown in Fig. 1. Moreover, due to edge relaxation, strains decrease rapidly in the barriers with increasing distance from the interfaces. For instance, at least 90% of the elastic energy in these layers is stored in the first few 20 nm on each side of the well for all structures discussed here (80 nm wide wires, 10 nm thick QW, and lattice mismatch close to 1%).

In order to compare different structures, we will define a relaxation ratio $\rho = 1 - \epsilon_{xx}^0 / \epsilon_{\parallel}$. Here ϵ_{xx}^0 is the strain ϵ_{xx} in the center of the wire and ϵ_{\parallel} the in-plane deformation before etching. Calculated values of ρ are more than 25% for 80 nm wide QWRs with 10 nm thick QWs for all the considered systems. Such a strain relaxation should indeed alter the optical properties of the structures. Let us now discuss the influence of the wire dimensions on the relaxation ratio ρ , namely the lateral width of the wire L_{QWR} , the thickness of the well L_{QW} , the distance h_b from the well to the unetched buffer, and the thickness h_c of the cap layer. One could expect the well and unetched buffer to interact significantly, which decreases ρ when reducing h_b . However, we have shown this decrease to be significant only for QWs very close to unetched material ($h_b < 2L_{QW}$), since most of the

elastic energy remains stored in the well and near the interfaces. Such situations rarely occur with experimental structures. In the same way, the thickness of the cap layer does not have much influence on the relaxation ratio as soon as $h_c > 2L_{QW}$. Therefore the most relevant dimensions having some influence on ρ appear to be the lateral width L_{QWR} of the wire and the thickness L_{QW} of the well. Since we did not find any nonlinear effects for structures down to $L_{QWR} \sim 10 \text{ nm}$, ρ should essentially depend on the “aspect ratio” $\chi = L_{QWR} / L_{QW}$ of the well.

The evolution of the relaxation ratio is reported in Fig. 4 for various structures. As we would expect, it decreases with increasing χ (that is, with increasing lateral width of the wires L_{QWR} or decreasing thickness of the well L_{QW}), since effective edge relaxation only occurs close to the sidewalls over a distance approximately twice the thickness of the well. As a consequence, strains are much more uniform in the well across the wire width in QWRs with higher aspect ratio χ .

On the other hand, the strain field becomes strongly non-uniform in the well both across the wire width and along the growth axis for wires with $\chi \leq 4$. We have found that the stress could even turn to an overrelaxation in the center of the wire when $\chi \leq 1.5$, which means $\rho > 1$. The well is then partly “overrelaxed” due to the bending of lattice planes. However, such cases should be considered separately since the distribution of elastic energy in these wires is far too inhomogeneous to be described by a single parameter such as ρ . Thus, we will now focus on wires with $\chi > 4$, which apply to most experimental structures.

It can be seen from Fig. 4 that the relaxation ratio ρ does not depend very much on the nature of the materials constituting the QWR. This curve $\rho(\chi)$ can be viewed, therefore, as a universal one as it directly applies to other various QWRs structures, as long as the elastic constants do not differ too much in the wells and the etched barriers. The relaxation ratio ρ appears to decrease as $1/(\chi + \chi_0)$ in the investigated range $4 \leq \chi \leq 32$, with $\chi_0 \sim 0.58$, which is small compared to χ .

Strain relaxation in the well will induce changes in band-gap energy and thus energy shifts of the optical transitions in these structures. We have calculated the total change ΔE of

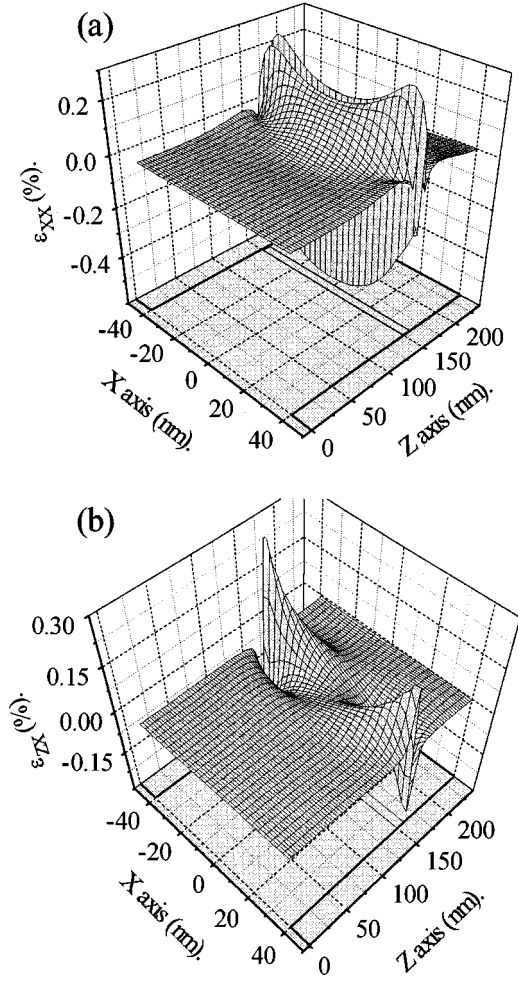


FIG. 2. Strain component ϵ_{xx} (a) and shear component ϵ_{xz} (b) in a CdTe QWR under compression plotted both across the wire width (x axis) and along the growth axis (z axis). The positions of the CdTe QW and of the sidewalls are shown in projection on the (xz) plane.

the band-gap energy in the well at $k=0$ by solving the Bir and Pikus strain Hamiltonian¹² in the $[110]$, $[1\bar{1}0]$, $[001]$ axis set:

$$\Delta E_{\pm} = a(\epsilon_{xx} + \epsilon_{yy} + \epsilon_{zz}) \pm \frac{1}{2} \sqrt{b^2(2\epsilon_{zz} - \epsilon_{xx} - \epsilon_{yy})^2 + d^2[(\epsilon_{xx} - \epsilon_{yy})^2 + (2\epsilon_{zx})^2]} \quad (1)$$

Here a , b , and d are deformation potentials taken from Refs. 5, 4, and 13 for CdTe, $\text{Zn}_{0.80}\text{Cd}_{0.20}\text{Se}$, and ZnTe, respectively. The first term is the effect of the hydrostatic pressure and the second one comes from tetragonal or trigonal distortions and shear deformation. For purely tetragonal distortion (e.g., for fully biaxially strained layers), the ground state ΔE_{-} corresponds to the ‘‘heavy,’’ $|\frac{3}{2}, \pm\frac{3}{2}\rangle$ (‘‘light,’’ $|\frac{3}{2}, \pm\frac{1}{2}\rangle$) hole and ΔE_{+} to the ‘‘light’’ (‘‘heavy’’) hole for compressive (tensile) deformation. In other cases, the energy eigenstates ΔE_{+} and ΔE_{-} are mixed states of the ‘‘light’’ and ‘‘heavy’’ holes.

We have computed the difference ΔE_{QWR} between the band-gap energy shift ΔE_{-} in fully biaxially strained QWs

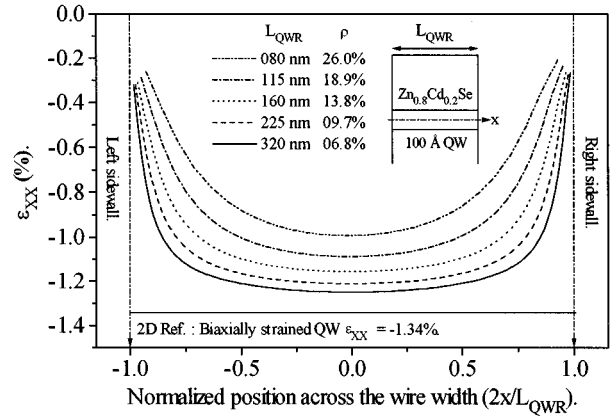


FIG. 3. Strain relaxation in $\text{Zn}_{0.80}\text{Cd}_{0.20}\text{Se}$ QWRs under compression with 10 nm thick QWs and various lateral widths L_{QWR} from 80 to 320 nm. The strain component ϵ_{xx} is plotted across the wire width in the middle of the $\text{Zn}_{0.80}\text{Cd}_{0.20}\text{Se}$ QW and the position in the well is normalized to the lateral width of the wire. The solid line labeled ‘‘2D Ref. : Biaxially strained QW’’ corresponds to the in-plane deformation in the well before etching.

and in the corresponding relaxed QWRs. The results are plotted in Fig. 5 for 80 nm wide $\text{Zn}_{0.80}\text{Cd}_{0.20}\text{Se}$, CdTe, and ZnTe wires with $L_{\text{QW}} = 10$ nm. We neglect any unidimensional (1D) effects (which should be negligible for $L_{\text{QWR}} = 80$ nm) and the confinement energies in QWs.

This figure shows a blue energy shift of the gap in the center of CdTe QWRs and a red energy shift in $\text{Zn}_{0.80}\text{Cd}_{0.20}\text{Se}$ QWRs as compared to the biaxially strained QW band gap. This different behavior is due to the relative values of the deformation potentials a and b in these two systems, which have an opposite contribution for the lowest band gap [see Eq. (1)]. Note that the band-gap energy of these two compressive layers tends towards the unstrained gap in the center of the wire as it relaxes strains. However, the band-gap energy abruptly decreases close to the sidewalls. This results from (i) a strong relaxation towards a uniaxial strained area and (ii) strong shear deformations.

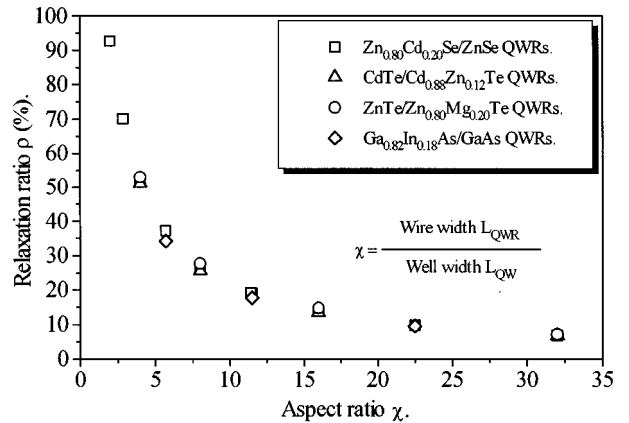


FIG. 4. Relaxation ratio versus aspect ratio of the wire. The results are reported for four different structures, e.g., CdTe, $\text{Zn}_{0.80}\text{Cd}_{0.20}\text{Se}$, and $\text{Ga}_{0.82}\text{In}_{0.18}\text{As}$ QWRs under compression, and ZnTe QWRs under tension. This curve $\rho(\chi)$ is applicable to many other structures (see text).

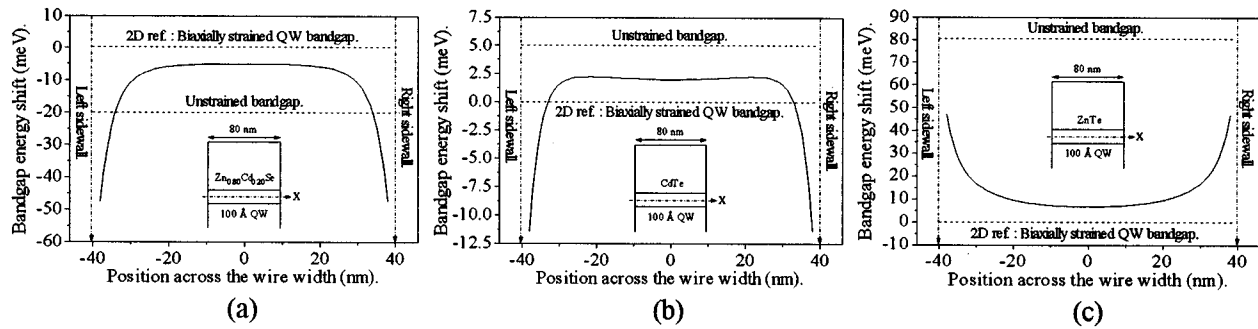


FIG. 5. Band-gap energy shifts in $\text{Zn}_{0.80}\text{Cd}_{0.20}\text{Se}$ (a) and CdTe (b) QWRs under compression, and in ZnTe (c) QWRs under tension ($L_{\text{QWR}} = 80$ nm, $L_{\text{QW}} = 10$ nm). The band-gap energy shift is plotted across the wire width in the middle of the well. The energy reference (dashed line labeled “2D Ref.: Biaxially strained QW band gap”) corresponds to the band-gap energy in the well before etching.

This could help diffusion of free carriers from the center of the wire towards its edges where they could be trapped on surface defects which are induced by the etching process.¹⁴ These etching defects could explain the strong decrease of the radiative efficiency observed in etched QWRs with decreasing lateral width. It is nevertheless difficult to treat this effect quantitatively, but it is worth noticing that the opposite behavior is expected for tensile layers such as in ZnTe QWRs; the band-gap energy increases close to the sidewalls and should prevent any important carrier diffusion to nonradiative surface defects.

If we assume that the photoluminescence (PL) energy lines lie close to the band-gap value in the central region of the wire, we can infer PL line shifts between unetched 2D QWs and etched QWRs. For $L_{\text{QWR}} = 80$ nm and $L_{\text{QW}} = 10$ nm we get a 6 meV redshift for $\text{Zn}_{0.80}\text{Cd}_{0.20}\text{Se}$ QWRs, a 2 meV blueshift for CdTe QWRs, and an 8 meV blueshift for ZnTe QWRs. This is in good agreement with experimental values given for CdTe (Ref. 5) and $\text{Zn}_{0.80}\text{Cd}_{0.20}\text{Se}$ (Ref. 4) wires, where a 2.5 meV blueshift and an 8 meV redshift were observed, respectively. Therefore, it is reasonable to assume that PL line shifts in etched quantum wires are due to local strain redistribution. Let us note finally that the shear strains which appear outside the center of the well generate a piezoelectric field. However, the influence on this piezoelectric potential on the position of the PL emission has been calculated¹⁵ to be typically 0.1 meV in the case of $\text{ZnSe}/\text{Cd}_x\text{Zn}_{1-x}\text{Se}$, and is safely negligible.

In summary, we have calculated inhomogeneous strain relaxation in etched quantum wires. We have shown how both tensile and compressive QWs tend to relax through the free surfaces, dragging the barriers and inducing deformations in these layers. We have studied the influence of wire dimensions on relaxation and have derived a “universal law” which displays how relaxation decreases with the aspect ratio of the wire $L_{\text{QWR}}/L_{\text{QW}}$. Moreover, by contrast to previous strain relaxation calculations,⁶ which assimilated the nanostructures to an isotropic elastic medium, our work, which is not based on such an assumption, validates (Fig. 4) these former works. Finally, we have found band-gap energy shifts due to strain redistribution in the wire for various II-VI semiconductors systems: for nanostructures under compression, this calculation accounts for the different behaviors observed in experimental data, whereas for nanostructures under tension, we expect a strong blueshift in $\text{ZnTe}/\text{Zn}_{0.80}\text{Mg}_{0.20}\text{Te}$ wires together with an increase of radiative efficiency, due to the larger band gap obtained on both sides of the wire as compared to the one in the center. This latter effect, which is induced by the inhomogeneous strain relaxation, is expected for most of the wires that undergo a tensile strain.

The authors thank G. Brunthaler for communicating preliminary results on the piezoelectric effect, and R. Cox (CEA-CNRS Grenoble) for his critical reading of the manuscript. This work has been partly supported by France Telecom (Contract No. 96 1B002).

¹A. Izrael *et al.*, Appl. Phys. Lett. **56**, 830 (1990).

²W. Walecki *et al.*, Appl. Phys. Lett. **57**, 2641 (1990).

³L. De Caro and L. Tapfer, Phys. Rev. B **51**, 4381 (1995).

⁴H. Straub *et al.*, J. Cryst. Growth **159**, 451 (1996); H. Straub *et al.*, XXIV International School of Physics of Semiconducting Compounds, Jaszowiec, 1996 [Acta Phys. Pol. A (to be published)].

⁵C. Gourgon *et al.*, in *Proceedings of the Nanostructures Physics and Technology International Symposium, St. Petersburg, 1996*, edited by Zh. Alferov and L. Esaki (Russian Academy of Sciences, St. Petersburg, 1996), p. 272.

⁶S. C. Jain *et al.*, J. Appl. Phys. **78**, 1630 (1995); D. Faux, *ibid.* **75**,

186 (1994); M. Grundmann *et al.*, Phys. Rev. B **50**, 14 187 (1994).

⁷P. N. Keating, Phys. Rev. **145**, 637 (1966).

⁸J. L. Martins and A. Zunger, Phys. Rev. B **30**, 637 (1984).

⁹M. Illing *et al.*, Appl. Phys. Lett. **67**, 124 (1995).

¹⁰M. Haase *et al.*, Appl. Phys. Lett. **59**, 1272 (1991).

¹¹Ch. Gréus *et al.*, Phys. Rev. B **47**, 7626 (1993).

¹²G. Bir and E. Pikus, Fiz. Tverd. Tela (Leningrad) **1**, 154 (1959) [Sov. Phys. Solid State **1**, 1502 (1960)].

¹³C. Van de Walle, Phys. Rev. B **39**, 1871 (1989).

¹⁴Y. S. Tang *et al.*, J. Appl. Phys. **77**, 6481 (1995).

¹⁵G. Brunthaler *et al.* (private communication).